

# Transport Properties of the Tomato Fruit Tonoplast<sup>1</sup>

## III. TEMPERATURE DEPENDENCE OF CALCIUM TRANSPORT

Received for publication August 17, 1987 and in revised form June 7, 1988

DARYL C. JOYCE<sup>2</sup>, GRANT R. CRAMER<sup>3</sup>, MICHAEL S. REID, AND ALAN B. BENNETT\*  
*Department of Environmental Horticulture (D.C.J., M.S.R.) and Department of Vegetable Crops, Mann Laboratory (G.R.C., A.B.B.), University of California, Davis, California 95616*

### ABSTRACT

Calcium transport into tomato (*Lycopersicon esculentum* Mill. cv Castlemart) fruit tonoplast vesicles was studied. Calcium uptake was stimulated approximately 10-fold by MgATP. Two ATP-dependent Ca<sup>2+</sup> transport activities could be resolved on the basis of sensitivity to nitrate and affinity for Ca<sup>2+</sup>. A low affinity Ca<sup>2+</sup> uptake system ( $K_m > 200$  micromolar) was inhibited by nitrate and ionophores and is thought to represent a tonoplast localized H<sup>+</sup>/Ca<sup>2+</sup> antiport. A high affinity Ca<sup>2+</sup> uptake system ( $K_m = 6$  micromolar) was not inhibited by nitrate, had reduced sensitivity to ionophores, and appeared to be associated with a population of low density endoplasmic reticulum vesicles that contaminated the tonoplast-enriched membrane fraction. Arrhenius plots of the temperature dependence of Ca<sup>2+</sup> transport in tomato membrane vesicles showed a sharp increase in activation energy at temperatures below 10 to 12°C that was not observed in red beet membrane vesicles. This low temperature effect on tonoplast Ca<sup>2+</sup>/H<sup>+</sup> antiport activity could only be partially ascribed to an effect of low temperature on H<sup>+</sup>-ATPase activity, ATP-dependent H<sup>+</sup> transport, passive H<sup>+</sup> fluxes, or passive Ca<sup>2+</sup> fluxes. These results suggest that low temperature directly affects Ca<sup>2+</sup>/H<sup>+</sup> exchange across the tomato fruit tonoplast, resulting in an apparent change in activation energy for the transport reaction. This could result from a direct effect of temperature on the Ca<sup>2+</sup>/H<sup>+</sup> exchange protein or by an indirect effect of temperature on lipid interactions with the Ca<sup>2+</sup>/H<sup>+</sup> exchange protein.

Calcium is widely acknowledged as an important second messenger in eukaryotic organisms (11, 18). Calcium fluxes have been associated with major changes in metabolism in plants and animals (11, 13), and it has also been proposed that transient fluctuations in cytoplasmic Ca<sup>2+</sup> activity may play a central role in chilling injury of chilling-sensitive plants (14, 21, 22). It is therefore of interest to obtain a complete understanding of mechanisms regulating subcellular Ca<sup>2+</sup> distribution in plant cells. ATP-dependent transport of Ca<sup>2+</sup> has been demonstrated in microsomal membrane preparations (9, 17, 24), in mitochondria (10), and in membrane fractions enriched in endoplasmic reticulum (5, 6, 8, 20) or tonoplast (8, 20).

In tomato fruit, Ca<sup>2+</sup> regulation has been implicated in the regulation of fruit softening (7), calmodulin-mediated protein

phosphorylation during fruit ripening (25), and in chilling injury (21, 22). Here we have investigated the mechanisms and temperature dependence of ATP-dependent Ca<sup>2+</sup> transport in a tonoplast enriched membrane fraction isolated from mature-green tomato fruit.

### MATERIALS AND METHODS

**Plant Material.** Mature green tomato (*Lycopersicon esculentum* Mill. cv Castlemart) were harvested from the field (summer) or greenhouse (winter) immediately prior to use. Fruits were sliced, the locular material removed, and the pericarp used for membrane isolation.

**Membrane Preparation.** A tonoplast-enriched membrane fraction from tomato was prepared as previously described (16), with minor modifications. Pericarp tissue (100 g) was homogenized in a chilled blender with 200 ml of 250 mM sucrose, 70 mM Tris/Mes (pH 8), 4 mM DTT, 3 mM EDTA, 0.1% (w/v) BSA, and 0.5% (w/v) soluble polyvinylpyrrolidone (PVP-40). The homogenate was filtered through cheesecloth and the filtrate centrifuged for 15 min at 13,000g in a Beckman SW 28 rotor at 4°C. The supernatant was retained and centrifuged at 80,000g for 45 min. The pellet was resuspended in 250 mM sucrose, 2 mM DTT, and 5 mM Tris/Mes (pH 7) and layered onto a discontinuous (16/26/34/40% w/v) or continuous (15-45% w/v) sucrose gradient containing 2 mM DTT and 5 mM Tris/Mes (pH 7). Sucrose gradients were centrifuged at 80,000g for 2 h. The tonoplast-enriched fraction was collected from the 16/26% (w/v) sucrose interface, diluted with an equal volume of 10 mM Tris/Mes (pH 7) and membranes pelleted at 80,000g for 30 min. The pellet was resuspended in 250 mM sucrose, 2 mM DTT, and 5 mM Tris/Mes (pH 7) to an average concentration of 1.6 mg protein/ml and frozen in liquid nitrogen. For the continuous sucrose gradient, 18 fractions (2 ml each) were collected and stored in liquid nitrogen until assayed. Beet tonoplast membranes were prepared as described (2).

**Calcium Transport Assays.** Calcium transport was assayed by measuring the uptake of radiolabeled Ca<sup>2+</sup> (<sup>45</sup>CaCl<sub>2</sub> was obtained from New England Nuclear [ $164 \times 10^7$  Bq/mg Ca<sup>2+</sup>] or Amersham [ $90 \times 10^7$  Bq/mg Ca<sup>2+</sup>]). The specific activity of <sup>45</sup>Ca<sup>2+</sup> ranged from  $30 \times 10^5$  to  $164 \times 10^7$  Bq/mg Ca<sup>2+</sup> in the assay, depending on the Ca<sup>2+</sup> concentration in the assay. Assays were conducted in 101  $\mu$ l volume containing 50 mM KCl, 6 mM MgSO<sub>4</sub>, 25 mM K<sub>2</sub>SO<sub>4</sub>, 3 mM Tris/ATP, 69 mM sucrose, 0.6 mM DTT, 1.4 mM Tris/Mes (pH 7) and approximately 20  $\mu$ g membrane protein. The water used in all reaction stocks was double deionized and passed through a Dowex 50 column to eliminate Ca<sup>2+</sup> contamination. Inhibitors soluble in methanol (*i.e.* A23187, valinomycin, nigericin, gramicidin, oligomycin, and DCCD<sup>4</sup>)

<sup>1</sup> Supported by National Science Foundation grant No. DMB 84-04990.

<sup>2</sup> Present address: Department of Agriculture, Baron-Hay Court, South Perth, W.A. 6151, Australia.

<sup>3</sup> Present address: Department of Plant Science, University of Nevada, Reno, NV 89557.

<sup>4</sup> Abbreviation: DCCD: *N,N'*-dicyclohexylcarbodiimide.

were added after membrane addition to a final methanol concentration of 0.1% (v/v). Assays were carried out in disposable polystyrene test tubes maintained at 28°C in a water bath. Except for the time course study, Ca<sup>2+</sup> uptake was measured after a 15 min incubation. The reaction was stopped by dilution with 4 ml of chilled 250 mM sucrose, 50 mM KCl, and 25 mM Tris/Mes (pH 7). The diluted vesicles were immediately filtered onto 0.45 μm Millipore HAWP filters, and the test tube and filter rinsed with an additional 4 ml of buffer. Filters were transferred to scintillation vials and radioactivity determined by liquid scintillation counting. For experiments determining temperature dependence of Ca<sup>2+</sup> uptake the temperature range was achieved using an aluminum temperature gradient block. The dimensions of the block were 13 cm wide, 8 cm high, and 60 cm long with 10 sets of 5 evenly spaced holes drilled along the top of the block and equipped with channels to allow temperature-regulated water to be circulated at either end of the block. After temperature equilibration the block maintained a linear temperature gradient whose endpoints were determined by the temperature of the water circulated at each end.

**Calcium Efflux.** Calcium retained in vesicles following passive efflux at different temperatures and time intervals was monitored. Vesicles were preloaded with <sup>45</sup>Ca<sup>2+</sup> by incubation at 28°C for 40 to 60 min in a medium containing 50 mM KCl, 25 mM K<sub>2</sub>SO<sub>4</sub>, 6 mM MgSO<sub>4</sub>, 3 mM ATP, 50 mM Hepes/Tris (pH 7), and 1 μM <sup>45</sup>Ca<sup>2+</sup>. Calcium loading was terminated by the addition of 95 μM EGTA and tubes then transferred to the appropriate temperature. At the indicated times the efflux assay was terminated and the Ca<sup>2+</sup> retained in the membrane vesicles was determined in the manner described for Ca<sup>2+</sup> uptake assays.

**H<sup>+</sup> Transport.** Development of interior acid pH gradients was monitored as the quenching of a fluorescent permeant amine dye (acridine orange) with a Perkin Elmer fluorescence spectrophotometer (16). Temperatures of the assays were controlled between 2 and 21°C with a circulating refrigerated water bath connected to the cuvette water jacket. Temperatures in the cuvette were monitored with a Cu/Cd thermocouple and microvoltmeter, using an ice bath reference. Approximately 47 and 150 μg membrane protein were used for individual tomato and red beet H<sup>+</sup> transport assays, respectively. The reaction medium was 50 mM KCl, 5 mM MgSO<sub>4</sub>, 222 mM sucrose, 4.5 mM Tris/Mes (pH 7), 1.8 mM DTT, and 3 mM Tris/ATP. Assays were started by addition of ATP, and quench of acridine orange fluorescence was monitored at excitation and emission wave lengths of 472 and 525 nm, respectively. Total quench (% *Q*) was measured as the proportion of full quench attained when the quench curve reached its minimum level. The initial rate of quench (% *Q* min<sup>-1</sup>) was estimated from the initial slope of the quench trace upon addition of ATP.

**Enzyme, Protein, and Chlorophyll Assay.** Nitrate and vanadate sensitive ATPase activities were measured as tonoplast and plasma membrane markers, respectively (2). ATPase activity was assayed at 28°C as previously described (16). The reaction contained 30 mM Tris/Mes (pH 6.5), 6 mM MgSO<sub>4</sub>, 50 mM KCl, 3 mM Tris/ATP, either 25 mM K<sub>2</sub>SO<sub>4</sub> or 50 mM KNO<sub>3</sub>, and 50 μM vanadate where indicated. The temperature range was achieved using the aluminum temperature gradient block described above.

Antimycin A-insensitive NAD(P)H-Cyt *c* reductase activity was assayed as an endoplasmic reticulum marker enzyme (12). The assay contained 47 mM phosphate buffer (pH 7.5), 0.8 mM NaCN, 7 μM antimycin A, 20 μM Cyt *c*, and 0.2 mM NADPH in 1.5 ml. The reaction was started by the addition of a 100 μl aliquot of membrane fraction and reduction of Cyt *c* measured at 550 nm.

UDPase activity was assayed as a marker for Golgi membranes (15). The reaction contained 0.1% (v/v) Triton X-100, 1.5 mM MnSO<sub>4</sub>, 30 mM bis-tris-propane/Mes (pH 7), and 1.5 mM UDP

in 0.5 ml. The reaction was run for 30 min at 28°C and liberation of inorganic phosphate determined by the method of Ames (1), except that 4% SDS (w/v) was included in the reagent to avoid interference by Triton X-100.

Protein was determined by the method of Schaffner and Weissman (19).

## RESULTS

Preliminary experiments were carried out with 0.7 μM <sup>45</sup>CaCl<sub>2</sub> to determine the time course of ATP-dependent Ca<sup>2+</sup> uptake in the tonoplast-enriched membrane fraction isolated from tomato fruit (Fig. 1). We have previously characterized a NO<sub>3</sub><sup>-</sup>-sensitive H<sup>+</sup>-ATPase associated with this membrane fraction (16) and others have characterized Ca<sup>2+</sup>/H<sup>+</sup> antiport activity in plant tonoplast preparations (4, 8, 20). Our results indicated that ATP stimulated Ca<sup>2+</sup> uptake approximately 10-fold and this uptake was reversible by the calcium ionophore, A23187. However, under the conditions employed, Ca<sup>2+</sup> uptake was stimulated rather than inhibited by NO<sub>3</sub><sup>-</sup>, suggesting that the uptake mechanism was not coupled to the activity of the NO<sub>3</sub><sup>-</sup>-sensitive tonoplast H<sup>+</sup>-ATPase.

When a wider range of Ca<sup>2+</sup> concentration was examined both NO<sub>3</sub><sup>-</sup>-sensitive and NO<sub>3</sub><sup>-</sup>-insensitive Ca<sup>2+</sup> uptake could be resolved (Fig. 2). At concentrations below 1 μM Ca<sup>2+</sup>, NO<sub>3</sub><sup>-</sup> either had no effect or stimulated Ca<sup>2+</sup> uptake (Figs. 1 and 2A). However, at concentrations above 10 μM Ca<sup>2+</sup>, the NO<sub>3</sub><sup>-</sup>-insensitive component of Ca<sup>2+</sup> uptake saturated and NO<sub>3</sub><sup>-</sup> inhibition of Ca<sup>2+</sup> uptake became evident (Fig. 2A). When a Hanes-Woolf plot of NO<sub>3</sub><sup>-</sup>-insensitive Ca<sup>2+</sup> uptake was plotted, a *K<sub>m</sub>* of approximately 6 μM Ca<sup>2+</sup> was estimated for this component of Ca<sup>2+</sup> uptake (Fig. 2B). To examine the NO<sub>3</sub><sup>-</sup>-sensitive component of Ca<sup>2+</sup> uptake, a much wider concentration range was employed (Fig. 2, C and D). Over this high concentration range, NO<sub>3</sub><sup>-</sup> inhibition of Ca<sup>2+</sup> uptake was evident and the Hanes-Woolf transformation of NO<sub>3</sub><sup>-</sup>-sensitive Ca<sup>2+</sup> uptake indicated a *K<sub>m</sub>* of approximately 250 μM (Fig. 2D).

Interestingly, we found that attempts to assay the high affinity (NO<sub>3</sub><sup>-</sup>-insensitive) component of Ca<sup>2+</sup> uptake in glass test tubes was confounded by high levels of Ca<sup>2+</sup> released from the glass surface. When assayed in the presence of 0.7 μM exogenous Ca<sup>2+</sup>, uptake was consistently lower when assayed in glass rather than

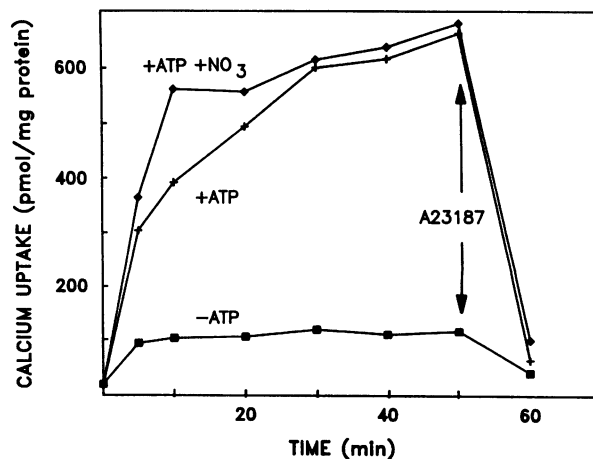


FIG. 1. Time course of Ca<sup>2+</sup> uptake by tonoplast-enriched membrane vesicles from tomato fruit. Uptake was measured in polystyrene test tubes at a Ca<sup>2+</sup> concentration of 0.7 μM in the absence (■) or presence (+) of 3 mM ATP or in the presence of 3 mM ATP and 50 mM KNO<sub>3</sub> (◇). When added, 50 mM KNO<sub>3</sub> replaced 25 mM K<sub>2</sub>SO<sub>4</sub> in the reaction medium. At 55 min, 5 μM A23187 was added to the reaction medium. Data are means of duplicate assays.

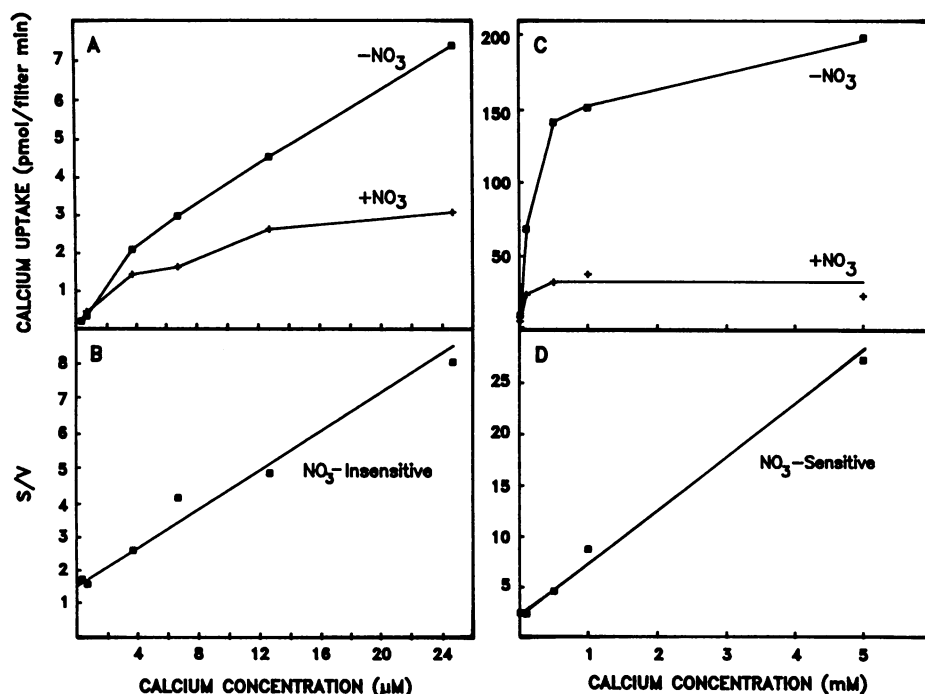


FIG. 2. Calcium concentration dependence of ATP-dependent  $\text{Ca}^{2+}$  uptake by tonoplast-enriched membrane vesicles from tomato fruit. Assays were carried out over the concentration range between 0.35 and 24.7  $\mu\text{M}$  (panel A) or between 50 and 5000  $\mu\text{M}$  (panel C). ATP-dependent  $\text{Ca}^{2+}$  uptake was determined as the difference between uptake in the absence and presence of 3 mM ATP; these are the values plotted. Over both concentration ranges  $\text{Ca}^{2+}$  uptake was measured in the absence and presence of 50 mM  $\text{KNO}_3$ . Data for  $\text{NO}_3^-$ -insensitive  $\text{Ca}^{2+}$  uptake over the low concentration range were determined as the uptake measured in the presence of 50 mM  $\text{KNO}_3$  and this data replotted using a Hanes-Woolf transformation (panel B).  $\text{NO}_3^-$ -sensitive  $\text{Ca}^{2+}$  uptake over the high concentration range was determined as the difference in uptake measured in the absence and presence of 50 mM  $\text{KNO}_3$  and this data replotted using a Hanes-Woolf transformation (panel D).

plastic test tubes. Furthermore,  $\text{NO}_3^-$  inhibited  $\text{Ca}^{2+}$  uptake when assayed in glass test tubes but stimulated  $\text{Ca}^{2+}$  uptake when assayed in plastic test tubes (data not shown). Based on the results shown in Figures 1 and 2 this difference between glass and plastic test tubes can be readily explained by the release of  $\text{Ca}^{2+}$  from the glass surface. This release of  $\text{Ca}^{2+}$  decreased the specific activity of  $^{45}\text{Ca}^{2+}$  in the reaction, leading to an apparent decrease in  $\text{Ca}^{2+}$  uptake rate and increased the  $\text{Ca}^{2+}$  concentration to a range where  $\text{NO}_3^-$  inhibition became apparent. We estimate that sufficient  $\text{Ca}^{2+}$  was released from glass test tubes to raise the  $\text{Ca}^{2+}$  concentration in the assay to approximately 20  $\mu\text{M}$ .

To further characterize the two components of ATP-dependent  $\text{Ca}^{2+}$  uptake, inhibitor sensitivity of  $\text{Ca}^{2+}$  uptake was determined at low (0.7  $\mu\text{M}$ ) or high (210  $\mu\text{M}$ )  $\text{Ca}^{2+}$  concentration (Table I). At high  $\text{Ca}^{2+}$  concentration uptake was strongly inhibited by  $\text{NO}_3^-$ , DCCD, and ionophores but was insensitive to

inhibition by vanadate or mitochondrial ATPase inhibitors,  $\text{N}_3$ , and oligomycin. In contrast, at low  $\text{Ca}^{2+}$  concentration  $\text{Ca}^{2+}$  uptake was stimulated by  $\text{NO}_3^-$ , inhibited by vanadate and DCCD, showed reduced sensitivity to ionophores but was similarly unaffected by the mitochondrial ATPase inhibitors,  $\text{N}_3$ , and oligomycin. These results indicate that the two  $\text{Ca}^{2+}$  uptake mechanisms can be distinguished on the basis of  $\text{Ca}^{2+}$  concentration dependence and inhibitor sensitivity. The  $\text{NO}_3^-$  and ionophore sensitivity of the low affinity  $\text{Ca}^{2+}$  uptake system suggests that this uptake represents the activity of a tonoplast localized  $\text{Ca}^{2+}/\text{H}^+$  antiport coupled to the activity of the  $\text{NO}_3^-$ -sensitive  $\text{H}^+$ -ATPase. This type of system has been characterized in several other tissues including red beet (4, 8, 20). For comparison, we also assayed  $\text{Ca}^{2+}$  uptake at high concentration in red beet tonoplast vesicles and found inhibitor characteristics almost identical to those of the low affinity  $\text{Ca}^{2+}$  uptake system in tomato fruit membrane vesicles (Table I). This supports our view that this system is indeed comparable to the  $\text{Ca}^{2+}/\text{H}^+$  antiport characterized in other systems. The high affinity system of  $\text{Ca}^{2+}$  uptake ( $\text{NO}_3^-$ -insensitive) had inhibitor characteristics similar to  $\text{Ca}^{2+}$ -ATPase-dependent  $\text{Ca}^{2+}$  uptake that has been localized to the endoplasmic reticulum in other tissues (8, 20).

To assess the subcellular localization of high affinity ATP-dependent  $\text{Ca}^{2+}$  uptake, a continuous sucrose gradient was analyzed (Fig. 3). Nitrate- and vanadate-sensitive ATPase activities were resolved on the gradient (panel B); however, the distribution of high affinity  $\text{Ca}^{2+}$  uptake (panel C) did not coincide with either ATPase activity, showed  $\text{NO}_3^-$ -stimulation rather than  $\text{NO}_3^-$ -inhibition in all fractions and showed a prominent low-density peak that would be expected to be collected with our tonoplast-enriched membrane fraction taken from a 16/26% sucrose interface. This low-density peak of high affinity  $\text{Ca}^{2+}$  uptake coincided with a low-density peak of NAD(P)H Cyt c reductase activity (panel D), suggesting that the high affinity  $\text{Ca}^{2+}$  uptake was localized in the endoplasmic reticulum. A second, high-density peak of NAD(P)H Cyt c reductase was not associated with a peak of  $\text{Ca}^{2+}$  uptake (panel D), suggesting the existence of density gradient-resolvable endoplasmic reticulum domains, only some of which possess high affinity  $\text{Ca}^{2+}$  uptake.

Because increases in cytoplasmic  $\text{Ca}^{2+}$  have been implicated

Table I. Effect of Inhibitors on  $\text{Ca}^{2+}$  Uptake in Tomato and Red Beet Tonoplast-Enriched Membrane Fractions

Calcium uptake was measured at 0.7 and 210  $\mu\text{M}$   $\text{Ca}^{2+}$  in the presence of the indicated inhibitors. All assays contained 0.1% methanol. Data are the means and standard deviations for duplicate assays from two independent experiments.

Inhibitor	$\text{Ca}^{2+}$ Uptake		
	Tomato		Red beet
	0.7 $\mu\text{M}$ $\text{Ca}^{2+}$	210 $\mu\text{M}$ $\text{Ca}^{2+}$	210 $\mu\text{M}$ $\text{Ca}^{2+}$
	% of control		
Control	100	100	100
+ $\text{NO}_3^-$ (50 mM)	126 $\pm$ 4	23 $\pm$ 5	29 $\pm$ 4
+Vanadate (50 $\mu\text{M}$ )	53 $\pm$ 6	99 $\pm$ 15	113 $\pm$ 14
+DCCD (100 $\mu\text{M}$ )	51 $\pm$ 8	10 $\pm$ 4	14 $\pm$ 2
+A23187 (5 $\mu\text{M}$ )	05 $\pm$ 5	10 $\pm$ 3	15 $\pm$ 5
+Nigericin (1 $\mu\text{M}$ )	70 $\pm$ 4	23 $\pm$ 9	21 $\pm$ 6
+Gramicidin (1 $\mu\text{M}$ )	77 $\pm$ 5	46 $\pm$ 15	52 $\pm$ 33
+Valinomycin (0.1 $\mu\text{M}$ )	104 $\pm$ 3	110 $\pm$ 4	182 $\pm$ 15
+ $\text{N}_3$ (200 $\mu\text{M}$ )	103 $\pm$ 4	103 $\pm$ 6	103 $\pm$ 6
+Oligomycin (1 $\mu\text{g}/\text{mL}$ )	101 $\pm$ 6	99 $\pm$ 11	114 $\pm$ 18

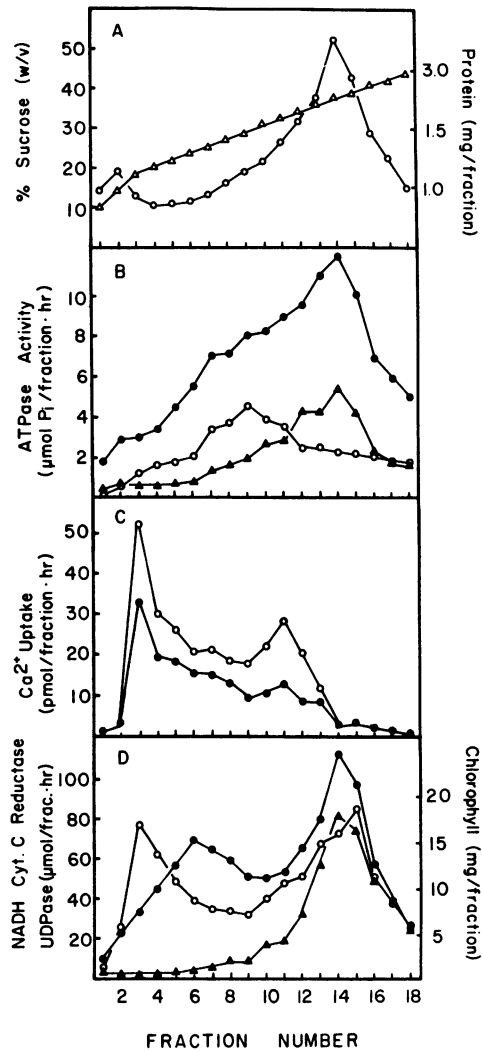


FIG. 3. Distribution of high affinity  $\text{Ca}^{2+}$  uptake activity and marker enzymes associated with tomato fruit microsomal membranes on a continuous sucrose gradient. Panel A, % sucrose (w/v) ( $\Delta$ ), and protein ( $\circ$ ); panel B, total ATPase activity ( $\bullet$ ),  $\text{NO}_3^-$ -sensitive ATPase activity ( $\circ$ ), and vanadate-sensitive ATPase activity ( $\blacktriangle$ ); panel C, ATP-dependent  $\text{Ca}^{2+}$  uptake in the absence ( $\bullet$ ) or presence ( $\circ$ ) of 50 mM  $\text{KNO}_3$ . Calcium uptake was measured at  $0.7 \mu\text{M} \text{Ca}^{2+}$ . Panel D, Chl ( $\blacktriangle$ ), UDPase activity ( $\bullet$ ), and NAD(P)H Cyt *c* reductase activity ( $\circ$ ).

as an early event in chilling injury (14, 21, 22) we assessed the temperature dependence of  $\text{Ca}^{2+}$  uptake in tonoplast-enriched vesicles from both tomato and red beet. Calcium uptake in tomato membrane vesicles was linear over a time course of 20 min at both high and low temperature (Fig. 4, insets). Calcium uptake in beet membrane vesicles was also linear (data not shown).

The data were plotted as an Arrhenius plot to reveal anomalous effects of temperature on  $\text{Ca}^{2+}$  uptake (Fig. 4). Calcium uptake in beet membranes showed a low temperature dependence with a relatively low activation energy. In contrast,  $\text{Ca}^{2+}$  uptake in tomato membrane vesicles had an activation energy similar to beet at high temperatures but this apparent activation energy increased significantly at temperatures below 10 to 12°C (Fig. 4). There is considerable controversy about the way to fit Arrhenius plots (14). We chose the simple approach by fitting with polynomial regression. The apparent energy of activation can be calculated by taking the derivative of the quadratic equation fit to the data. Clearly this model is not perfect, partic-

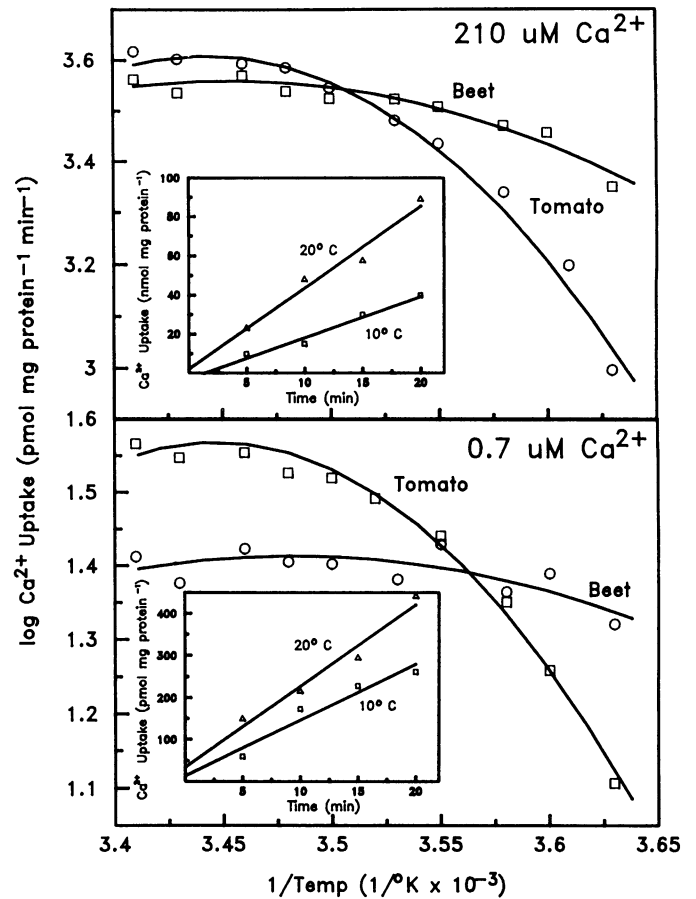


FIG. 4. Arrhenius plots of the temperature-dependence of ATP-dependent  $\text{Ca}^{2+}$  uptake at 0.7 and  $210 \mu\text{M} \text{Ca}^{2+}$  by red beet and tomato tonoplast-enriched membrane vesicles. Curves were fit by polynomial regression. Equations for the polynomial fit were:  $0.7 \mu\text{M} \text{Ca}^{2+}$ , beet ( $-40.297 + 23.955x - 3.44x^2$ );  $0.7 \mu\text{M} \text{Ca}^{2+}$ , tomato ( $-152.955 + 89.669x - 13.009x^2$ );  $210 \mu\text{M} \text{Ca}^{2+}$ , beet ( $-66.175 + 40.378x - 5.845x^2$ );  $210 \mu\text{M} \text{Ca}^{2+}$ , tomato ( $-190.38 + 112.674x - 16.361x^2$ ). Insets are  $\text{Ca}^{2+}$  uptake in tomato membrane vesicles over the time course of the experiments at both low and high temperatures. Each data point is the mean of 3 replicates.

ularly at the high temperature range of the fit. It is, however, suitable for our purposes in contrasting the two genotypic responses.

Because the low affinity  $\text{Ca}^{2+}$  uptake system represents a complex reaction consisting of  $\text{H}^+$  transport driven by the  $\text{H}^+$ -ATPase and subsequent  $\text{Ca}^{2+}/\text{H}^+$  exchange, the effect of low temperature could be exerted at any of a number of sites in the reaction sequence. We examined the temperature dependence of individual steps in the reaction sequence by first assaying ATPase activity in the tomato and red beet membrane fractions (Fig. 5). The assays were carried out at saturating and half-saturating ATP concentrations as determined for each enzyme previously (3, 16). Both ATPases had similar activation energies that showed no apparent changes over the temperature range examined. Thus, the low temperature effects on  $\text{Ca}^{2+}$  uptake in tomato membranes cannot be attributed to an effect of temperature on the  $\text{H}^+$ -ATPase, at least as assessed by ATP hydrolytic activity.

The temperature dependence of  $\text{H}^+$  transport catalyzed by the tomato and red beet  $\text{H}^+$ -ATPase was also examined using the fluorescent,  $\Delta\text{pH}$  probe, acridine orange (Fig. 6). In both membranes the initial rate of  $\text{H}^+$  transport was greatly reduced when temperature was decreased from 21 to 6°C. However, the total extent of  $\Delta\text{pH}$  formation was similar at both temperatures. The

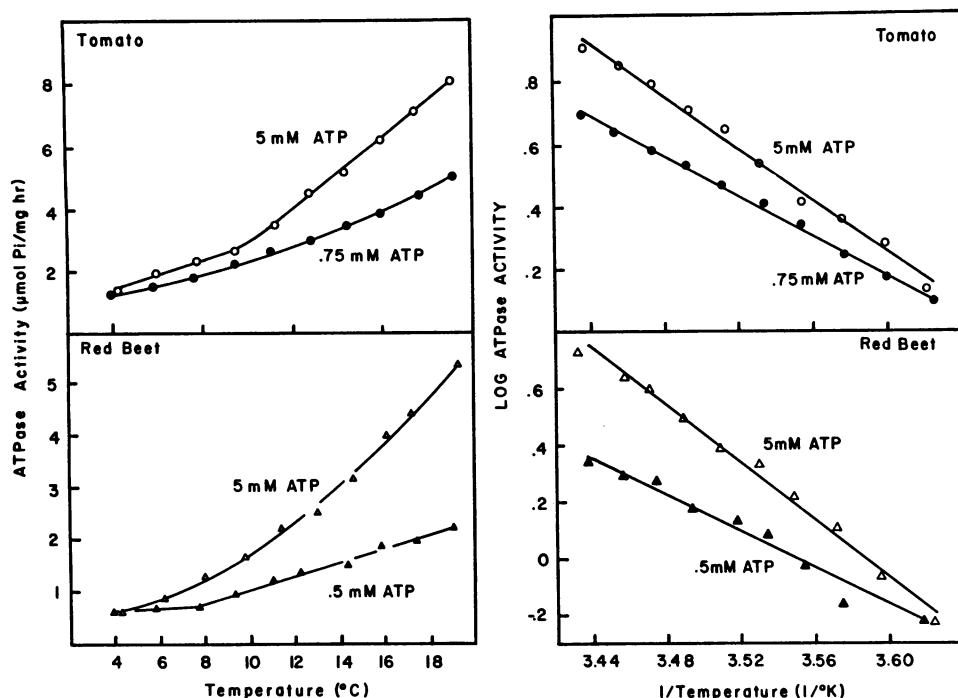


FIG. 5. Temperature-dependence of ATPase activity associated with tonoplast-enriched membrane fractions from red beet and tomato fruit. ATPase activity was assayed at the indicated temperature in the presence of saturating (5 mM) or half-saturating (0.5 mM-beet, 0.75 mM-tomato) ATP concentration. The data were transformed and Arrhenius plots of the data constructed.

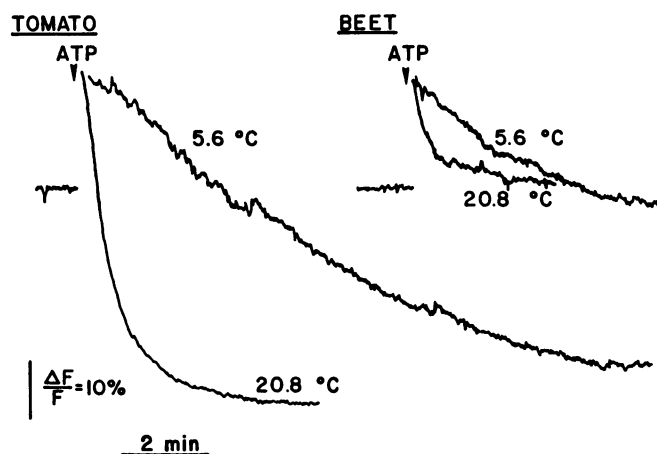


FIG. 6. ATP-dependent  $H^+$  transport activity associated with tonoplast-enriched membranes isolated from tomato or red beet. Proton transport was assayed using the fluorescent  $\Delta pH$  probe acridine orange and either 47  $\mu g$  (tomato) or 150  $\mu g$  (beet) membrane protein as described in "Materials and Methods." Temperature was regulated using a refrigerated water bath and a water-jacketed cuvette.

temperature dependence of the initial rate of  $H^+$  transport over the temperature range of 3 to 21°C is shown in Figure 7. An Arrhenius plot of the data (Fig. 7B) does not indicate sufficiently large enough changes in the activation energy for  $H^+$  transport to account for the low temperature effect on  $Ca^{2+}$  uptake. Because low temperature may induce ion leaks we also examined the extent of  $\Delta pH$  formation (*i.e.* total fluorescence quench) over the same temperature range (Fig. 8). The extent of  $\Delta pH$  formation was only slightly temperature dependent. We interpret the extent of  $\Delta pH$  formation to reflect the steady state balance between the rate of active  $H^+$  influx and the rate of passive  $H^+$  efflux. Because the steady state  $\Delta pH$  changed only slightly over a temperature range where the rate of active  $H^+$  influx changes dramatically, we conclude that passive  $H^+$  efflux decreased approximately in parallel with the decrease in active  $H^+$  influx activity. This indicates that both tomato and beet membrane vesicles become less permeable to  $H^+$  as the temperature de-

creases. Overall, decreases in  $\Delta pH$  cannot completely account for the low temperature effect on  $Ca^{2+}$  uptake in tomato membranes, because there is only a 21% reduction in steady state  $\Delta pH$  formation, whereas  $Ca^{2+}$  transport in the tonoplast was reduced by 62%.

The effect of low temperature on passive  $Ca^{2+}$  efflux was also examined by preloading vesicles with  $^{45}Ca^{2+}$  and measuring  $Ca^{2+}$  retention at time intervals after the addition of EGTA (Figs. 9 and 10). Initial experiments examined  $Ca^{2+}$  efflux after 20 min incubation at a range of temperatures (Fig. 9). As with passive  $H^+$  efflux, passive  $Ca^{2+}$  efflux progressively decreased with decreasing temperature. This was also observed when passive  $Ca^{2+}$  efflux was measured over a 3 h time period (Fig. 10). For both tomato and beet membranes, passive  $Ca^{2+}$  efflux was reduced at 5°C relative to 20°C. These results indicate that low temperature decreases rather than increases passive  $Ca^{2+}$  efflux and so a temperature effect on this process contributing to net  $Ca^{2+}$  uptake cannot account for the low temperature reduction of  $Ca^{2+}$  uptake in tomato membrane vesicles.

## DISCUSSION

Our results indicate that low-density membrane vesicles isolated from tomato fruit possess two mechanisms for ATP-dependent  $Ca^{2+}$  uptake. Calcium transport across the tonoplast appears to involve a  $Ca^{2+}/H^+$  antiport coupled to activity of the  $H^+$ -ATPase. This conclusion is based on  $NO_3^-$ -sensitivity and ionophore-sensitivity of the low affinity, high capacity uptake system. Similar tonoplast-localized  $Ca^{2+}/H^+$  antiport systems have been described in oat (20), carrot (8), and red beet (4). Our results differ somewhat in that we find a  $K_m$  for  $Ca^{2+}$  uptake by this system to exceed 200  $\mu M$  whereas two other papers report a  $K_m$  near 10  $\mu M$  (8, 20). This discrepancy may be due to difficulty in controlling  $Ca^{2+}$  concentration as we observed when glass test tubes were used.

The high affinity, low capacity uptake system appears to be associated with a subpopulation of endoplasmic reticulum membranes. A similar system has also been reported to be associated with endoplasmic reticulum of other plant cells (8, 20). Vanadate sensitivity of this uptake system suggests that a  $Ca^{2+}$ -ATPase may be the mechanism responsible for  $Ca^{2+}$  uptake by this

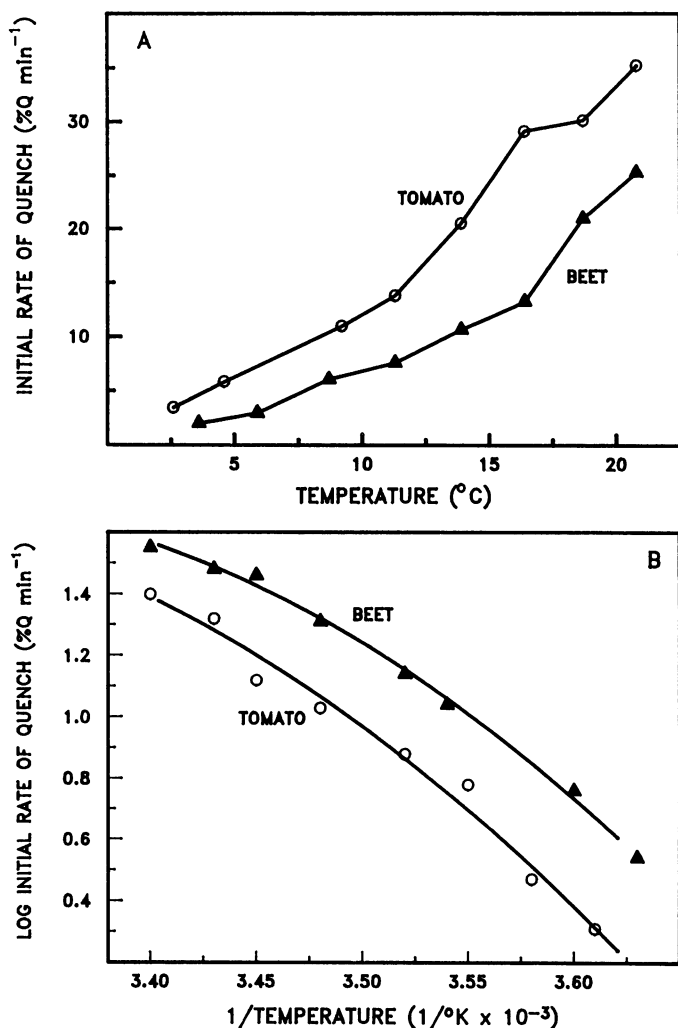


FIG. 7. Temperature-dependence of the initial rate of ATP-dependent  $H^+$  transport associated with tonoplast enriched membranes isolated from tomato or red beet. The initial rate of fluorescence quenching of acridine orange was determined from data similar to that shown in Figure 7, at the indicated temperature and plotted (panel A). The data in panel A were transformed and an Arrhenius plot constructed with curves fitted by polynomial regression (panel B).

system. Nitrate-stimulation of the rate of  $Ca^{2+}$  uptake by the high affinity system (see Fig. 1) may result from charge-compensating flux of  $NO_3^-$  which would suggest that the putative  $Ca^{2+}$ -ATPase catalyzes electrogenic  $Ca^{2+}$  influx. Similarly, valinomycin stimulation of low affinity  $Ca^{2+}/H^+$  antiport activity, especially in red beet membranes (Table I) suggests that this system may be electrogenic as well.

The presence of both intracellular  $Ca^{2+}$  uptake systems may provide complementary mechanisms that operate in concert to regulate cytoplasmic  $Ca^{2+}$  activity. The systems could be likened to mechanisms of coarse and fine controls, with the low affinity, high capacity tonoplast system responsive to relatively large transients in  $Ca^{2+}$  activity and the high affinity, low capacity endoplasmic reticulum system responsive to more subtle perturbations in cytoplasmic  $Ca^{2+}$  levels.

The temperature dependence of  $Ca^{2+}$  uptake in low density beet and tomato membrane vesicles indicated that the apparent activation energy for  $Ca^{2+}$  uptake increased in tomato membranes at temperatures below 10 to 12°C (Fig. 4). Thus, in the event of chilling-induced increases in cytoplasmic calcium, restoration of  $Ca^{2+}$  homeostasis may be delayed in tomato relative

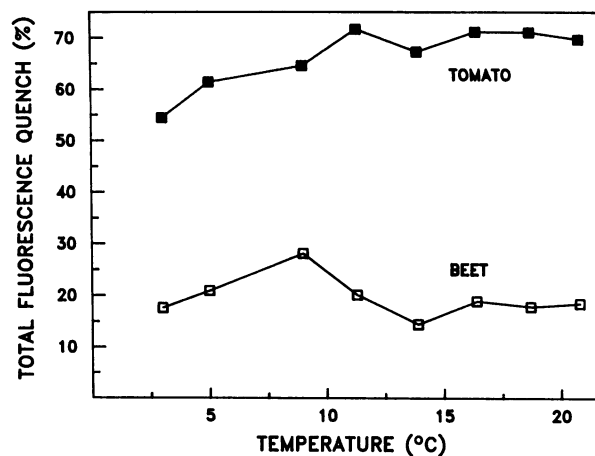


FIG. 8. Temperature-dependence of the extent of  $\Delta pH$  formation in tonoplast-enriched membranes isolated from tomato or red beet. The total fluorescence quench of acridine orange was determined from data similar to that shown in Figure 7, at the indicated temperatures.

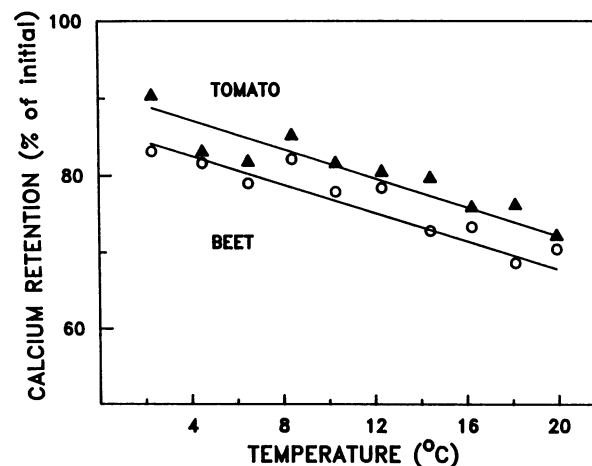


FIG. 9. Temperature-dependence of passive  $Ca^{2+}$  efflux from tonoplast-enriched membranes isolated from tomato or red beet. Membrane vesicles were loaded by preincubation in  $1 \mu M$   $^{45}Ca^{2+}$ , then  $95 \mu M$  EGTA was added to the solution, and the membranes transferred to the indicated temperature. After 20 min the  $Ca^{2+}$  retained in membrane vesicles was determined using the filtration assay as described in "Materials and Methods."

to red beet. To elucidate the mechanism of this low temperature effect on  $Ca^{2+}$  uptake in low density tomato membranes we examined the temperature dependence of components of the reaction contributing to  $Ca^{2+}/H^+$  antiport activity in the tonoplast. Temperature did not affect ATPase activity,  $H^+$  transport activity, passive  $H^+$  fluxes or passive  $Ca^{2+}$  fluxes to the same extent as the low temperature effect on  $Ca^{2+}$  uptake. Considered collectively, these results argue that a general loss of compartmentation resulting from low temperature effects on membrane structure can only account for a minor portion of the inhibition of  $Ca^{2+}$  uptake. The results suggest that the major effect of low temperature on  $Ca^{2+}$  transport results from an effect of low temperature directly on the  $Ca^{2+}/H^+$  exchange reaction. Three possible explanations for the major effect of low temperature-induced change in activation energy for the  $Ca^{2+}/H^+$  exchange reaction are: (a) structural changes in the membrane microdomain or boundary lipid associated with the carrier complex may have occurred, (b) temperature may directly affect a conformation state of the  $Ca^{2+}/H^+$  exchange protein, or (c) temperature may exert differential effects on rate constants of serial steps

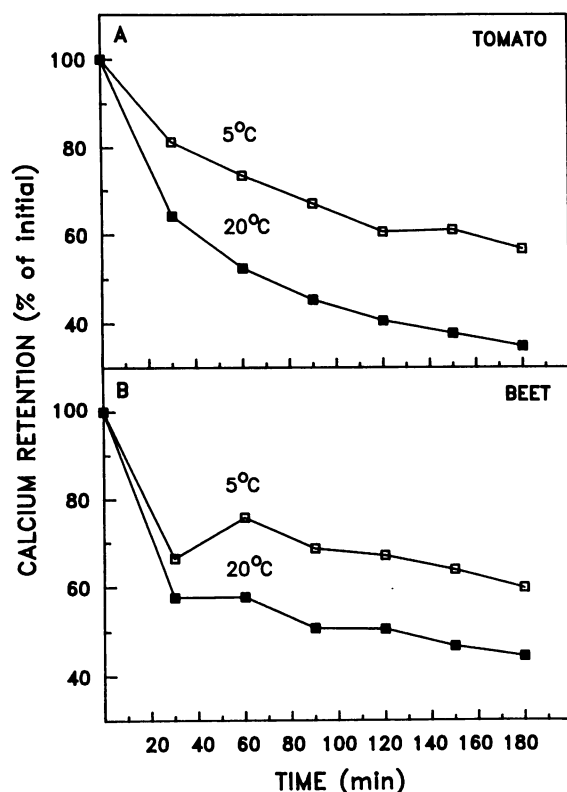


FIG. 10. Time course of  $\text{Ca}^{2+}$  efflux from tonoplast-enriched membrane vesicles isolated from tomato or red beet. Membrane vesicles were passively loaded by preincubation with  $1 \mu\text{M}$   $^{45}\text{Ca}^{2+}$ , then  $95 \mu\text{M}$  EGTA was added to the solution, and the test tubes with the membranes were transferred to temperatures of either 5 or  $20^\circ\text{C}$ . At the indicated times the  $\text{Ca}^{2+}$  retained in membrane vesicles was determined using the filtration assay as described in "Materials and Methods."

involved in  $\text{Ca}^{2+}/\text{H}^+$  exchange and thus alter the rate limiting step of the overall reaction.

The present study does not identify a source for the postulated chilling-induced  $\text{Ca}^{2+}$  fluxes into the cytoplasm of chilling sensitive cells (14, 21, 22). However, a direct effect of temperature in inducing  $\text{Ca}^{2+}$  fluxes from either the mitochondria (10) or vacuole now appear to be unlikely sources of a chill-induced  $\text{Ca}^{2+}$  transient. The plasma membrane remains a candidate since Zocchi and Hanson (23) found that corn root tissue exposed to a chilling shock absorbed appreciably more  $\text{Ca}^{2+}$  than control roots. The possibility also exists that chilling-induced  $\text{Ca}^{2+}$  efflux from intracellular stores may be mediated by products of phosphatidylinositol catabolism, such as inositol triphosphate (13). The apparent increase in activation energy for  $\text{Ca}^{2+}$  transport into intracellular compartments that we observed in tomato could exacerbate a chill-induced increase in cytoplasmic  $\text{Ca}^{2+}$  by increasing the duration of cytosolic exposure to elevated  $\text{Ca}^{2+}$  activity.

## LITERATURE CITED

- AMES BN 1966 Assay of inorganic phosphate, total phosphate, and phosphatases. *Methods Enzymol* 8: 115-118
- BENNETT AB, SD O'NEILL, RM SPANSWICK 1984  $\text{H}^+$ -ATPase activity from storage tissue of *Beta vulgaris*. I. Identification and characterization of an anion-sensitive  $\text{H}^+$ -ATPase. *Plant Physiol* 74: 538-544
- BENNETT AB, SD O'NEILL, M EILMANN, RM SPANSWICK 1985  $\text{H}^+$ -ATPase activity from storage tissue of *Beta vulgaris*. III. Modulation of ATPase activity by reaction substrates and products. *Plant Physiol* 78: 495-499
- BLUMWALD E, RJ POOLE 1986 Kinetics of  $\text{Ca}^{2+}/\text{H}^+$  antiport in isolated tonoplast vesicles from storage tissue of *Beta vulgaris* L. *Plant Physiol* 80: 727-731
- BUCKHOUT TJ 1983 ATP-dependent  $\text{Ca}^{2+}$  transport in purified endoplasmic reticulum membrane vesicles from *Lipidium sativum* L. roots. *Plant Physiol* 159: 84-90
- BUCKHOUT TJ 1984 Characterization of  $\text{Ca}^{2+}$  transport in purified endoplasmic reticulum membrane vesicles from *Lipidium sativum* L. roots. *Plant Physiol* 76: 962-967
- BUESCHER RW, GE HOBSON 1982 Role of calcium and chelating agents in regulating the degradation of tomato fruit tissue by polygalacturonase. *J Food Biochem* 6: 147-160
- BUSH DR, H SZE 1986 Calcium transport in tonoplast and endoplasmic reticulum vesicles isolated from cultured carrot cells. *Plant Physiol* 80: 549-555
- DIETER P, D MARME 1980 Calmodulin activation of plant microsomal  $\text{Ca}^{2+}$  uptake. *Proc Natl Acad Sci USA* 77: 7311-7314
- FERGUSON IB, MS REID, RJ ROMANI 1985 Effects of low temperature and respiratory inhibitors on calcium flux in plant mitochondria. *Plant Physiol* 77: 877-880
- HEPLER PK, RO WAYNE 1985 Calcium and plant development. *Annu Rev Plant Physiol* 36: 397-439
- HODGES TK, RT LEONARD 1974 Purification of a plasma membrane-bound adenosine triphosphatase from plant roots. *Methods Enzymol* 32: 392-406
- HOCHACHKA PW 1986 Defense strategies against hypoxia and hypothermia. *Science* 231: 234-241
- MINORSKY PV 1985 An heuristic model of chilling injury in plants: a role for calcium as the primary physiological transducer of injury. *Plant Cell Environ* 8: 75-94
- NAGAHASHI J, AP KANE 1982 Triton-stimulated nucleoside diphosphatase activity: subcellular localization in corn root homogenates. *Protoplasma* 112: 167-173
- OLESKI N, P MAHDAVI, G PEISER, AB BENNETT 1987 Transport properties of the tomato fruit tonoplast. I. Identification and characterization of an anion-sensitive  $\text{H}^+$ -ATPase. *Plant Physiol* 84: 993-996
- RASI-CALDOGNO F, MI DEMICHELIS, MC PUGLIARELLO 1982 Active transport of  $\text{Ca}^{2+}$  in membrane vesicles from pea: evidence for a  $\text{H}^+/\text{Ca}^{2+}$  antiport. *Biochem Biophys Acta* 693: 287-295
- ROUX SJ, RO WAYNE, N DATTA 1986 Role of calcium ions in phytochrome responses: an update. *Plant Physiol* 66: 344-348
- SCHAFFNER WC, C WEISSMAN 1973 A rapid, sensitive, and specific method for the determination of protein in dilute solution. *Anal Biochem* 56: 502-514
- SCHUMAKER KS, H SZE 1985 A  $\text{Ca}^{2+}/\text{H}^+$  antiport system driven by the proton electrochemical gradient of a tonoplast  $\text{H}^+$ -ATPase from oat roots. *Plant Physiol* 79: 1111-1117
- WOODS CM, VS POLITO, MS REID 1984 Response to chilling stress in plant cells. II. Redistribution of intracellular calcium. *Protoplasma* 121: 17-24
- WOODS CM, MS REID, BD PATTERSON 1984 Response to chilling stress in plant cells. I. Changes in cyclosis and cytoplasmic structure. *Protoplasma* 121: 8-16
- ZOCCHI G, JB HANSON 1982 Calcium influx into corn roots as a result of cold shock. *Plant Physiol* 70: 318-319
- ZOCCHI G, JB HANSON 1983 Calcium transport and ATPase activity in a microsomal membrane vesicle fraction from corn roots. *Plant Cell Environ* 6: 203-209
- VELUTHAMBI K, BW POOVAIAH 1984 Calcium-promoted protein phosphorylation in plants. *Science* 223: 167-169